Int. J. Heat Mass Transfer. Vol. 36, No. 3, pp. 695–703, 1993
Printed in Great Britain

0017-9310/93 $6.00 + 0.00
© 1993 Pergamon Press Ltd

On droplet evaporation in the presence of a condensing substance: the effect of internal diffusion

T. VESALA

Department of Physics, University of Helsinki, Siltavuorenpenger 20 D, SF-00170, Helsinki, Finland

(*Received* 2 *January* 1992)

Abstract—Evaporation and condensation of a continuum regime binary droplet accompanied by internal diffusion are investigated numerically. The evaluation of the mole fractions at the droplet surface is based on the model where a thin, well-stirred liquid film resulting from evaporation and condensation is allowed to mix with the droplet by diffusion in short time intervals. The effect of the internal diffusion on the evaporation rate of an ammonia droplet in the presence of condensing water vapour is examined. In particular, the evolution of the droplet temperature and the vapour pressure of ammonia just above the droplet surface is investigated. The influence of the significant surface dilution of ammonia on the evaporation rate is reduced because of the increased droplet temperature which results from the decreased evaporation rate.

INTRODUCTION

THE UNDERSTANDING of condensational growth and evaporation of particles is essential in many atmospheric and environmental studies and in many branches of technological applications, such as in chemical engineering. Generally, these processes depend on the capability of the gas phase to transfer vapour molecules, and this mass transfer is coupled by heat transfer resulting from the heat released in condensation and consumed in evaporation. The outward mass and heat fluxes depend on the boundary values (vapour pressure and temperature) far from the droplet surface and just above it. The former are determined by external conditions, the latter are governed by internal transfer processes, which are coupled with outward transfer processes. In order to estimate the evaporation or growth rate of a droplet, the effect of the intrinsic transfer processes on boundary values should be investigated.

The problem of multicomponent (two or more components) droplet evaporation and condensation is substantially more complicated than the problem of one component droplet, for several phenomena must be taken into account (e.g. ref. [1]). This study is devoted to the significance of the internal diffusion in binary (two-component) droplet evaporation in the continuum regime (macroscopic transfer processes). No internal convective flow is allowed for. The temperature within the droplet is taken to be spatially uniform, but temporally varying ignoring the effect of the droplet thermal capacity. For other investigations on mass and heat transport within multicomponent evaporating droplet, the reader may wish to refer to, e.g. refs. [2–4].

Numerical results for an ammonia droplet evaporating in the humid air at 20°C are presented in this study. As the temperature of the evaporating droplet is low, the evaporation is accompanied by the simultaneous condensation of water vapour at the droplet surface (the possible nucleation of water vapour owing to the low temperature gas around the droplet is neglected). In the conditions considered here, the evaporation and condensation proceed at a relatively fast rate and thus the ammonia–water droplet might display a sensitivity to the internal diffusion. The evolution of ammonia droplets in the dry air and in the humid air without internal diffusion (well-mixed behaviour) has been considered in refs. [5, 6], respectively.

THEORY

Gas-phase mass fluxes and droplet temperature

In order to calculate droplet evaporation, it is necessary to determine the gas-phase mass fluxes (the rates at which masses of species pass from or to the droplet surface), and the actual droplet temperature. The objective of this section is only to present some general aspects of the theory by which the mass fluxes and the droplet temperature are estimated. For more detailed description (expressions for mass fluxes and for droplet temperature; physico-chemical properties required for the model computations) the reader may wish to refer to ref. [6] (see also refs. [7, 8]).

Since the vapour diffusion and heat conduction in the gas proceed on a much faster time scale than growth or evaporation, the vapour concentrations and the temperature profiles near the droplet approach steady state before appreciable growth or evaporation occurs, and the gas-phase mass and heat fluxes can be considered as quasi-steady. Changes in

NOMENCLATURE

a	droplet radius
C	mass concentration
C_s	mass concentration in well-stirred liquid film (Fig. 1)
C_v	initial value of C_s
D_l	liquid phase diffusion coefficient
d	relative integration step
f, f_0	parameters in expression (6) for mass concentration
I	gas-phase mass flux
m_l	mass in the droplet
M	total mass of solute
M_i	molecular weight of species i
P	variable used in the Laplace transform
r	radial distance
R	dimensionless distance
s	variable used in the Laplace transform, $-s^2 \equiv P$
s_n	nth positive non-zero root of equation (4)
t	time
u	dimensionless variable, definitions (A4)
U	Laplace transformed dimensionless variable u
u_s	dimensionless mass concentration
V_0, V_s	volume of well-stirred liquid film (Fig. 1)
X	mole fraction.

Greek symbols

α_s, α	ratio of film volume to droplet volume (Fig. 1)
ρ	density
τ	dimensionless time
χ	mass fraction.

Subscripts

i	integration step
1	species
2	species.

these processes are determined by the changing boundary conditions. The validity of this statement has been investigated by numerous authors (e.g. ref. [9]).

Mass transfer results from ordinary molecular diffusion if there is no gradient in the total pressure and no external forces, and if thermal diffusion can be neglected (e.g. ref. [10]). The steady-state mole fraction gradient of a species due to ordinary diffusion, for a multicomponent ideal vapour mixture, is given by the well-known Stefan–Maxwell equations [11]. Kalkkinen *et al.* [7] have solved the differential Stefan–Maxwell equations analytically for a binary droplet evaporating in the presence of an inert gas. The solution produces non-linear algebraic equations for the constant mass fluxes, which can be solved numerically, if the droplet temperature and the mole fractions at the droplet surface are known. In this study, the expression presented by Kalkkinen *et al.* [7] are applied according to ref. [6].

An equation for the steady state droplet temperature can be derived using the energy conservation: the temperature (or the evaporation and condensation rates) levels off at a value where the phase transition heats can be transferred in the gas. The heats are transported by thermal conduction according to the Fourier's law, by diffusion as a result of the enthalpies carried by vapours, and by thermal radiation (e.g. ref. [12]). The direct effect of the concentration gradients (the Dufour effect) is usually of minor importance, and it is not taken into account here. Kulmala and Vesala [8] have derived an expression for the temperature of the one-component droplet, assuming that the thermal conductivity of the surrounding gas and the vapour enthalpy vary linearly with the temperature. In this study, the generalized multicomponent expression based on the former one is applied according to ref. [6] (see also ref. [13]). The expression includes also the corrections caused by the radiative heat transport in a transparent gas and by the excess mixing enthalpies resulting from non-ideal behaviour of the liquid mixture.

Internal concentration profile

The effect of relatively small liquid phase diffusivities causes the surface composition to differ from the bulk, less volatile species (if both species evaporate), condensing species (if the other species evaporates and another condenses) or species with higher condensation rate (if both species condense) tending to accumulate on the droplet surface. We approximate for convenience that this accumulation takes place in a well-stirred liquid solution at the droplet surface and consider diffusion from this well-mixed liquid solution into the droplet. In this stage, the well-stirred solution is restricted only to have limited volume. In the actual numerical model the solution volume is required to be small compared with the droplet volume.

Suppose that the droplet occupies the space $r \leqslant a$, while the volume of the well-stirred solution (excluding the space occupied by the droplet) is V_0. The concentration C_s of solute (accumulating species) in the solution is uniform. The solution and the droplet are assumed to be in the equilibrium. A schematic diagram of the system is presented in Fig. 1.

The concentration C at a distance r from the centre of the droplet is determined by the well-known unsteady diffusion equation in a spherically symmetric geometry

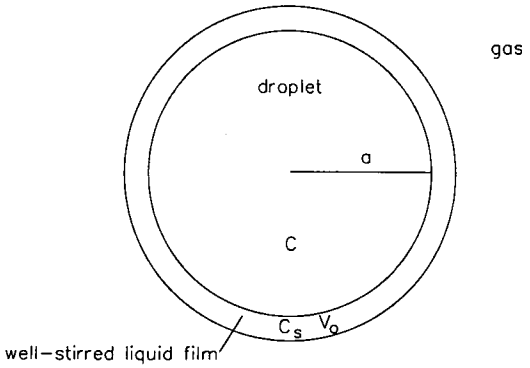

FIG. 1. Schematic diagram of the system. A well-stirred liquid film is mixed with the droplet by diffusion.

$$\frac{\partial rC}{\partial t} = D_l \frac{\partial^2 rC}{\partial r^2}, \quad r < a$$
$$C = C_s, \qquad r = a \tag{1}$$

where D_l is the liquid phase diffusion coefficient which is assumed to be constant as are the temperature and thermodynamic properties. Actually, the diffusion coefficient is a function of the concentration and thus also of the radial distance. For liquid mixtures, the binary diffusion coefficients are strongly concentration dependent (e.g. ref. [14]). However, there are relatively few experimental data of diffusion coefficient in liquids since measurements are tedious, and molecular theory does not succeed in describing the complicated processes in non-ideal liquid solutions with sufficient accuracy for predicting coefficients (e.g. ref. [15]). The concentration dependence is neglected here. If the mole fraction dependence is available, the approximate dependence can be included in calculations later. Note that equation (1) is written in the form which resembles the diffusion equation in one dimension.

First, let the initial concentration of the solute in the droplet be zero and in the well-mixed solution be C_v

$$C = 0, \quad t = 0, \quad r < a$$
$$C_s = C_v, \quad t = 0. \tag{2}$$

The behaviour of the system is similar to the conductive heating or cooling of a solid sphere in a well-stirred fluid investigated by Paterson [16] and the concentration of solute within the droplet is given by [16, 17]

$$C = \frac{M_0}{(4\pi a^3/3 + V_0)} + 2\frac{M_0}{V_0}\sum_{n=1}^{\infty} \frac{a}{r} \frac{\exp\left(\frac{-s_n^2 D_l t}{a^2}\right)\sin(rs_n/a)}{\left(\frac{3(\alpha+1)}{\alpha} + \frac{s_n^2\alpha}{3}\right)\sin s_n} \tag{3}$$

where M_0 is the total mass of solute and s_n is the nth positive non-zero root of

$$s\cot s = 1 + \frac{\alpha s^2}{3}. \tag{4}$$

The parameter α is the ratio of the volume of the solution and the droplet

$$\alpha = \frac{V_0}{4\pi a^3/3}. \tag{5}$$

The first three roots of equation (4) are presented by Paterson [16] for a wide range of α.

Now, the solution for the concentration profile introduced above is used as the initial concentration in a generalized case. Note that the solution for the concentration would be similar to equation (3) in respect to the dependence on the radial distance, although the initial concentration in the droplet would have been non-zero constant in equation (2). Thus, the generalized case describes the evolution of the intrinsic concentration profile for the droplet, which is initially composed of one species, or well-mixed (or its initial concentration profile depends on the radial distance according to equation (3)) (see the next section).

Consider the solution of the diffusion equation (1) when the initial concentration is given by

$$C = f_0 + \frac{a}{r}\sum_{n=1}^{\infty} f_n \sin(rs_n/a), \quad t = 0, r < a$$
$$C_s = C_v, \qquad t = 0 \tag{6}$$

according to equation (3). Parameters f_0 and f_n do not depend on the radial distance r. Let the volume of the solution be V_s and the corresponding ratio of the volume of the solution to the volume of the droplet be α_s.

The analytical solution of equation (1) with the above initial values can be obtained applying the Laplace transform and expanding the transformed solution in partial fractions in order to carry out the inverse transformation. Generally, this solution would depend both on α (by means of the parameter f_n) and on α_s, the actual ratio of the solution volume and the droplet. However, assuming that the volume ratios have the same values ($\alpha_s = \alpha$), the solution for the concentration profile becomes significantly simpler to use. The consequences of this assumption will be discussed in the next section.

We obtain for the concentration profile within the droplet (see Appendix)

$$C = \frac{M}{\frac{4\pi a^3}{3} + V_s} + \sum_{n=1}^{\infty}\left[\frac{2\left(\frac{M}{V_s} - \frac{(\alpha+1)f_0}{\alpha}\right)}{\left(\frac{3(\alpha+1)}{\alpha} + \frac{\alpha s_n^2}{3}\right)\sin s_n} + f_n\right]\frac{a}{r} \times \exp\left(\frac{-s_n^2 D_l t}{a^2}\right)\sin\left(\frac{rs_n}{a}\right) \tag{7}$$

where M is the total mass of the solute.

When $t \to \infty$

$$C \to \frac{M}{\frac{4\pi a^3}{3} + V_s}$$

and when $f_0 \to 0$ and $f_n \to 0$, the above equation reduces to the form of equation (3), as it is required. The series no doubt always converges [16]. However, the rapidity of convergence varies markedly with the parameter $s_n^2 D_1 t/a^2$. For low values of this parameter, the alternative solution by means of the error function (erf) is given by Paterson [16] corresponding to expression (3).

MODEL

Coupling of composition profile with mass fluxes and estimation of surface mole fractions

The quasi-steady evaporation (or condensation) rate of the droplet can be calculated according to the equation

$$\mathrm{d}t = -\frac{\mathrm{d}(m_{11}+m_{12})}{I_1+I_2} \tag{8}$$

where I_1 and I_2 are the gas-phase mass fluxes and m_{11} and m_{12} are the masses of species in the droplet. The minus sign comes from the sign convection (the mass flux is positive for an evaporating species).

We have carried out the integration of the evaporation time using extended trapezoidal rule (e.g. ref. [18]) by means of summing up changes in time (time intervals) as a function of changes in the mass of species 1

$$m_{11,i+1} - m_{11,i} \equiv \mathrm{d}m_{11,i} = m_{11,i}(\mathrm{d}_i - 1) \tag{9}$$

where d_i is the relative change in the mass 1 after time t_i. For the evaporating species, it is below unity. The change of the mass of species 2 $\mathrm{d}m_{12}$ is connected with the change of the mass of species 1 by

$$\mathrm{d}m_{12} = \frac{I_2}{I_1}\mathrm{d}m_{11}. \tag{10}$$

Unsophisticated as the extended trapezoidal rule is, it is in fact a fairly robust way of doing integrals of functions that are not very smooth [18].

The relative changes d_i in the mass 1 are determined by means of the volume ratio α (the ratio of the volume of the well-stirred solution and the droplet) so that the volume ratio is constant (i.e. $\alpha_s = \alpha$) all the time. The well-stirred solution on the droplet surface is produced by steady evaporation and condensation rates during each time interval.

In the following it is described step by step how the coupling of the unsteady concentration distributions with quasi-stationary mass fluxes has been modelled. It is assumed that species 1 is evaporating.

Phase I. Consider the droplet after time t_i, when its radius is a_i and the concentration of species 2 inside the droplet is given by $C_2(t_i, a_i)$. The concentration increases toward the droplet surface, because the species 2 is the condensing or less volatile substance.

Phase II. Because of evaporation during a small time interval, the droplet radius changes to a', but otherwise the concentration profile is assumed to remain the same. Phases I and II are shown schematically in Fig. 2(a). Note that in this stage the masses do not obviously conserve. However, the computer model keeps count of the exact amounts of the masses otherwise, and the part of the model described here represents only the approximate behaviour of the intrinsic concentration profiles.

Phase III. During the time interval, the liquid film of pure species 2 with the mass $m_{f2,e} + \mathrm{d}m_{12,i}$ is produced by evaporation of species 1 and by evaporation or condensation of species 2. The contribution $m_{f2,e}$ resulting from evaporation of species 1 is assumed to be the mass which corresponds to the change of the mass of species 1 ; i.e.

$$m_{f2,e} = \mathrm{d}m_{11,i}\frac{\chi_{1a,i} - 1}{\chi_{1a,i}}, \tag{11}$$

where $\chi_{1a,i}$ is the mass fraction of species 1 at the droplet surface after the time t_i. Taking into account also the contribution $\mathrm{d}m_{12,i}$ resulting from evaporation or condensation of species 2, we can write for α the expression

$$\alpha = \frac{\rho_{l,i}(\mathrm{d}m_{12,i} + m_{f2,e})}{\rho_{l2}(m_{11,i} + m_{12,i} + \mathrm{d}m_{11,i} - m_{f2,e})} \tag{12}$$

where $\rho_{l,i}$ is the overall density of the droplet and ρ_{l2} the density of the species 2 in liquid phase.

Phase IV. The concentration is allowed to change according to equation (7) during the time interval $t_{i+1} - t_i$. The roots of equation (4) are calculated by NAG-library FORTRAN-routine C05AZF [19]. Those terms which contribute less than 0.01% to the series are omitted. Phases III and IV are shown schematically in Fig. 2(b).

Phase V. Finally, the concentration profile is assumed to extend to the droplet surface and the procedure can be carried out again, Fig. 2(c). In this stage the masses do not conserve as before in phase II.

The relative changes d_i in the mass 1 are determined now so that the ratio of the film volume to the droplet volume remains constant. Using equations (9)–(12), we obtain

$$\mathrm{d}_i = 1 + \frac{\alpha\rho_{l2}(m_{11,i} + m_{12,i})}{m_{11,i}\rho_{l,i}\left(1 + \frac{I_{2,i}}{I_{1,i}} - \frac{1}{\chi_{1a,i}} + \frac{\alpha\rho_{l2}}{\rho_{l,i}\chi_{1a,i}}\right)}. \tag{13}$$

Because the absolute accuracy of the numerical integration method used remains unknowable, the effect of the value of the volume ratio α on the value

of the evaporation time has to be studied. The relative change in the evaporation time t_d is typically of the order of 1 or 0.1%, when the value of the volume ratio α changes from 0.01 to 0.001 or from 0.001 to 0.0001, respectively. In this study we use the order of 0.001, which gives for d_i the order of 0.99 during the greatest part of the droplet evolution. Note that the smaller value of the volume ratio corresponds to the smaller value of the mass change and further to a larger amount of time intervals. However, the larger amount of the time intervals does not always imply higher accuracy in the integration, because accumulated roundoff errors may start increasing.

Finally, the mole fractions at the droplet surface can be estimated by means of the concentration profile 7. The ratio of the surface concentration C_2 to the concentration at the well-mixed limit $C_2(D_1 \to \infty)$ is equal to the ratio of the surface mole fraction to the mole fraction at the well-mixed limit. Thus the mole fraction at the droplet surface is

$$X_{21,a} = X_{21,mix} \frac{C_2}{C_2(D_1 \to \infty)}, \tag{14}$$

where

$$X_{21,mix} = \frac{m_{12}}{m_{12} + \frac{M_2}{M_1} m_{11}}. \tag{15}$$

The mole fraction of species 1 can be calculated by

$$X_{11,mix} = 1 - X_{21,mix}. \tag{16}$$

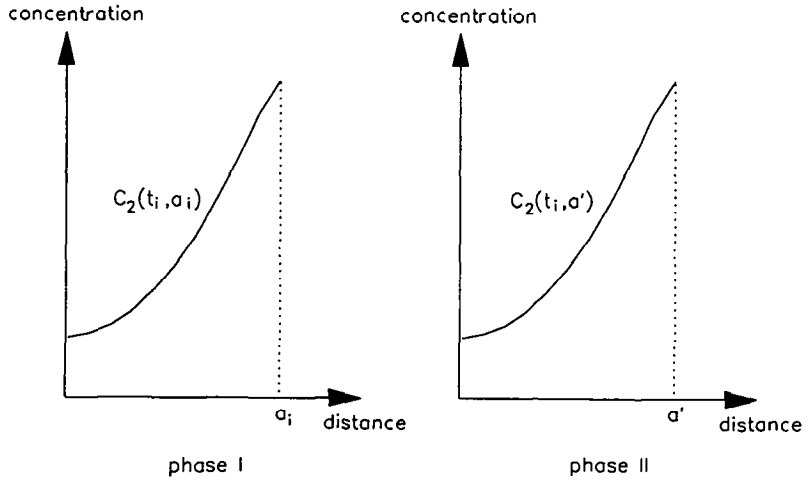

FIG. 2(a). The model for the coupling of the unsteady concentration distributions with quasi-stationary mass fluxes, phases I and II.

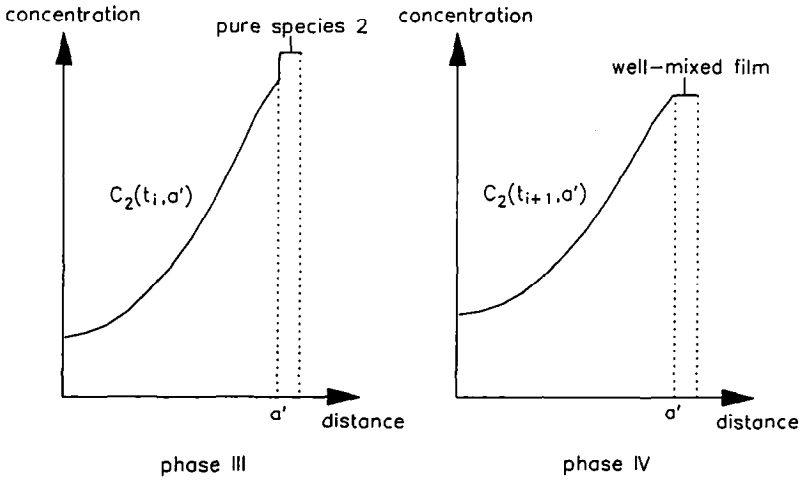

FIG. 2(b). The model for the coupling of the unsteady concentration distributions with quasi-stationary mass fluxes, phases III and IV.

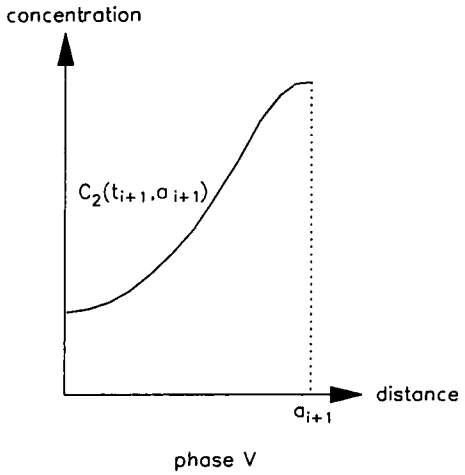

FIG. 2(c). The model for the coupling of the unsteady concentration distributions with quasi-stationary mass fluxes, phase V.

RESULTS

The evolution of an ammonia–water droplet

The model has been applied to predict the evolution of an ammonia–water droplet in humid air. The effect of the internal diffusion on the rate of evaporation of an ammonia droplet is examined. In particular, the evolution of the droplet temperature and the vapour pressure of ammonia just above the droplet surface is investigated.

Figure 3 shows the sensitivity of the evaporation rate of an initially pure ammonia droplet to the liquid phase diffusion coefficient. The coefficient has values 0.5×10^{-9}, 10^{-9} and 5×10^{-9} m^2 s^{-1}. Diffusion coefficients for most of the common organic and inorganic materials in the usual solvents, such as water, lie in the range from 0.3 to 1.5×10^{-9} m^{-2} s^{-1} [20]. The rate has also been calculated at the rapid mixing limit using an 'infinite' diffusion coefficient. The gas temperature is 20°C and the vapour pressure of ammonia in the gas is negligible. The relative humidity is 100%. The evaporation rate of the droplet is slightly decreased with decreasing liquid phase diffusion coefficient due to the dilution of ammonia at the droplet surface. After the time of 1.2 s, about 10% from the initial mass of ammonia is left in the droplet.

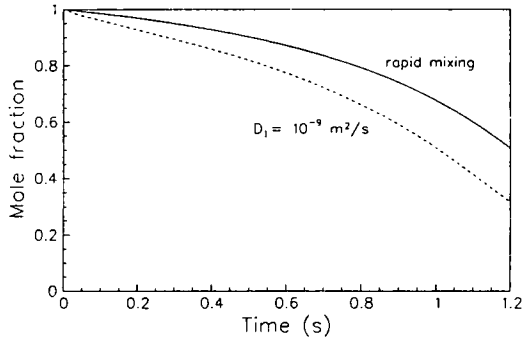

FIG. 4. The effect of the internal diffusion on the mole fraction of ammonia at the droplet surface. Finite liquid phase diffusion coefficient is 10^{-9} m^2 s^{-1}. The initial droplet radius, the gas temperature and the vapour pressure of ammonia and water in the gas are the same as in Fig. 3.

Figure 4 shows the mole fraction of ammonia at the droplet surface as a function of time. Liquid phase diffusion coefficient has the value 10^{-9} m^2 s^{-1}. The result calculated using this value can be compared with the result calculated using the rapid mixing model. The mole fraction given by the rapid mixing model is significantly higher. However, the effect of the dilution on the evaporation rate is not as significant according to Fig. 3.

Figure 5 shows the droplet temperature vs time. In every instant, the temperature (or the evaporation and condensation rates) has levelled off at a value where the phase transition heats can be transferred in the gas. Smaller evaporation rate due to the dilution tends to raise the droplet temperature, and therefore the saturation vapour pressure of ammonia at the droplet surface tends to increase. The effect of the dilution on the evaporation rate is reduced because of increased

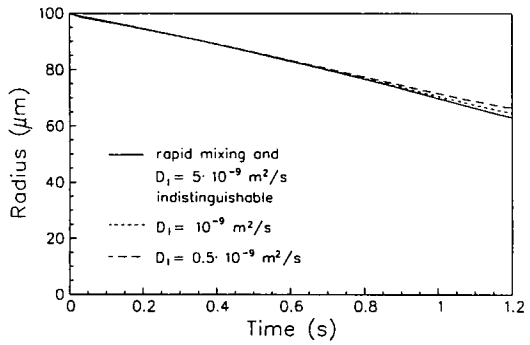

FIG. 3. The effect of the liquid phase diffusivity on the rate of evaporation of a freely falling, initially pure ammonia droplet. The gas temperature is 20°C and the vapour pressure of ammonia in the gas is negligible. The relative humidity is 100%.

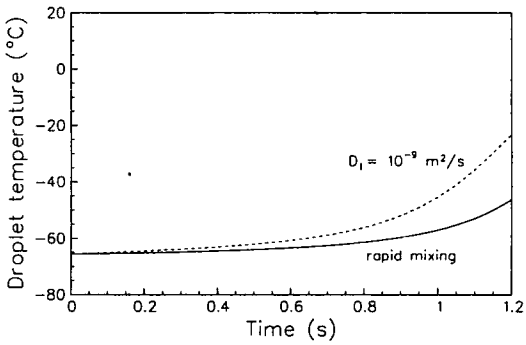

FIG. 5. The effect of the internal diffusion on the droplet temperature. Finite liquid phase diffusion coefficient is 10^{-9} m^2 s^{-1}. The initial droplet radius, the gas temperature and the vapour pressure of ammonia and water in the gas are the same as in Fig. 3.

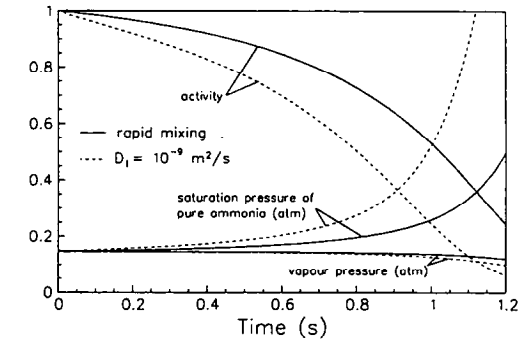

FIG. 6. The effect of the internal diffusion on the activity of ammonia at the droplet surface, on the saturation vapour pressure of pure ammonia at the droplet temperature and on the vapour pressure of ammonia just above the droplet surface. Finite liquid phase diffusion coefficient is 10^{-9} m^2 s^{-1}. The initial droplet radius, the gas temperature and the vapour pressure of ammonia and water in the gas are the same as in Fig. 3.

droplet temperature. Note that the droplet temperature is so low that the saturation vapour pressure of water is approximately zero, and thus the dilution has no significant direct effect on the mass flux of water vapour.

The vapour pressure of ammonia just above the droplet surface is given as a product of the liquid phase activity (the product of the liquid phase mole fraction and the activity coefficient) and the pure saturation vapour pressure (e.g. ref. [6]). The activity gives an indication of how 'active' a substance is relative to its pure saturation vapour pressure. Figure 6 shows the above quantities as a function of time. The pressures are given as fractions of atmospheric pressure. Note that the saturation vapour pressure increases exponentially with temperature. The liquid phase activity may be four times larger at the rapid mixing limit than with the value 10^{-9} m^2 s^{-1}. However, the combined effect of the increased droplet temperature and the dilution on the vapour pressure is small, which is consistent with the results presented in Fig. 3.

Finally, Fig. 7 shows the internal mole fraction profile of ammonia as a function of the radial distance after 0.3, 0.6, 0.9 and 1.2 s. The profile has not enough time to become flat. However, the mole fraction of ammonia in the droplet centre decreases substantially. We can say that the liquid phase diffusion proceeds on the same time scale as the evaporation process. This is consistent with the simple analysis by means of the characteristic time it takes for the dissolved species to diffuse throughout the entire droplet, since this time is of the same order of magnitude as the characteristic time for the droplet growth or evaporation [21].

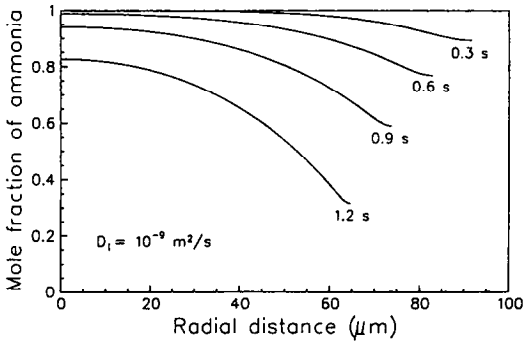

FIG. 7. The mole fraction of ammonia within the droplet as a function of the radial distance after 0.3, 0.6, 0.9 and 1.2 s. Liquid phase diffusion coefficient is 10^{-9} m^2 s^{-1}. The initial droplet radius, the gas temperature and the vapour pressure of ammonia and water in the gas are the same as in Fig. 3.

DISCUSSION AND CONCLUSIONS

The effect of the internal diffusion on the evaporation of an ammonia droplet in humid air was investigated and the main objective has been to clarify the significance of the internal diffusion in the droplet evaporation or condensation. The evaluation of the mole fractions at the droplet surface is based on the model where a thin, well-stirred liquid film is allowed to mix with the droplet by diffusion during short time intervals. This liquid film results from the quasi-steady evaporation and condensation processes. Somewhat simplified as this model is, it does not mask the nature of the physical processes involved in the droplet evolution. In ref. [13], the model predictions were compared with the numerical calculations, by Landis and Mills [2], for the evaporation of a heptane–octane droplet with the steady-state heat transfer. The obtained droplet behaviours were consistent.

According to the model calculations, the evaporation rate of ammonia decreases with decreasing liquid phase diffusion coefficient resulting from the dilution of ammonia at the droplet surface. However, if the typical value 10^{-9} m^2 s^{-1} for the diffusion coefficient is employed, the difference between the evaporation rates is small compared with the rapid mixing limit (infinite diffusion coefficient). The effect of the significant surface dilution is reduced because of the increased droplet temperature which results from the decreased evaporation rate. Although the real situations (finite and infinite diffusion coefficients) differ substantially from each other, the effects of dilution and temperature changes quite strongly compensate each other. This point has not been stressed in the literature. Note that this sort of 'negative feedback' effect is not due to the applied internal diffusion model, but is associated with the inherent physics of the processes. This conclusion indicates the need for measuring the surface properties of an evaporating multicomponent droplet, a fact that is also emphasized in the recent investigation by Aggarwal *et al.* [4].

Finally, it is useful to estimate the characteristic times associated with internal diffusion and droplet growth or evaporation. According to both simple analysis and numerical simulations, the ratio of the characteristic times for the droplet evaporation and for the internal diffusion is constant for all droplet

sizes in the continuum regime. Thus the qualitatively similar results presented in this study are obtained for all droplet sizes in the continuum regime if the species and the external conditions (temperature and partial vapour pressures) do not change. If the evaporation and condensation proceed at a relatively slower rate and the internal diffusion at the same rate, the diffusion has smaller effect, and the assumption of the well-mixed droplet is justified.

Acknowledgements—The financial support from the Academy of Finland is gratefully acknowledged. The author is also very pleased to acknowledge Dr Markku Kulmala of the Department of Physics and Mr Markus Olin of the Reactor Laboratory in the Technical Research Centre of Finland for stimulating discussions and for the significant help.

REFERENCES

1. P. Ravindran and E. Davis, Multicomponent evaporation of single aerosol droplets, *J. Colloid Interface Sci.* **85,** 278–288 (1982).
2. R. B. Landis and A. F. Mills, Effect of internal diffusional resistance on the evaporation of binary droplets. In *Fifth Int. Heat Transfer Conf. Proc.*, 3–7 September 1974, Tokyo, Vol. 4, Paper B7.9, pp. 345–349 (1974).
3. A. Y. Tong and W. A. Sirignano, Multicomponent droplet vaporization in a high temperature gas, *Combust. Flame* **66,** 221–235 (1986).
4. S. K. Aggarwal, G. Chen, T. A. Jackson and G. L. Switzer, Vaporization behavior of fuel droplets in a hot air stream, *Int. J. Heat Mass Transfer* **34,** 2669–2673 (1991).
5. J. Kukkonen, T. Vesala and M. Kulmala, The interdependence of evaporation and settling for airborne freely falling droplets, *J. Aerosol Sci.* **20,** 749–763 (1989).
6. T. Vesala and J. Kukkonen, A model for binary droplet evaporation and condensation, and its application for ammonia droplets in humid air, *Atmos. Environ.* **26A,** 1573–1581 (1992).
7. J. Kalkkinen, T. Vesala and M. Kulmala, Binary droplet evaporation in the presence of an inert gas: an exact solution of the Maxwell–Stefan equations, *Int. Commun. Heat Mass Transfer* **18,** 117–126 (1991).
8. M. Kulmala and T. Vesala, Condensation in the continuum regime, *J. Aerosol Sci.* **22,** 337–346 (1991).
9. D. E. Rosner and W. S. Chang, Transient evaporation and combustion of a fuel droplet near its critical temperature, *Combust. Sci. Technol.* **7,** 145–158 (1973).
10. J. O. Hirschfelder, C. F. Curtiss and R. B. Bird, *Molecular Theory of Gases and Liquids.* Wiley, New York (1954).
11. C. F. Curtiss and J. O. Hirschfelder, Transport properties of multicomponent gas mixtures, *J. Chem. Phys.* **17,** 550–555 (1949).
12. R. B. Bird, W. E. Stewart and E. N. Lightfoot, *Transport Phenomena.* Wiley, New York (1960).
13. T. Vesala, Binary droplet evaporation and condensation as phenomenological processes, Ph.D. Thesis, University of Helsinki, Department of Physics. *Commentationes Physico-Mathematicae et Chemico-Medicae*, Vol. 127. The Finnish Society of Sciences and Letters, Helsinki (1991).
14. R. K. Ghai, H. Ertl and F. A. L. Dullien, Liquid diffusion of nonelectrolytes: Part I, *A.I.Ch.E. Jl* **19,** 881–900 (1973).
15. W. Baldauf and H. Knapp, Experimental determination of diffusion coefficients, viscosities, densities and refractive indexes of 11 binary liquid systems, *Ber. Bunsenges. Phys. Chem.* **87,** 304–309 (1983).
16. S. Paterson, The heating or cooling of a solid sphere in a well-stirred fluid, *Proc. Phys. Soc.* **59,** 50–58 (1947).
17. J. Crank, *The Mathematics of Diffusion.* Oxford University Press, London (1957).
18. W. H. Press, B. P. Flannery, S. A. Teukolsky and W. T. Vetterling, *Numerical Recipes.* Cambridge University Press, New York (1986).
19. FORTRAN-routine C05AZF, *The NAG Fortran Library Manual—Mark 13*, Vol. 1. Numerical Algorithms Group, Oxford (1988).
20. T. K. Sherwood, *Absorption and Extraction* (1st Edn). McGraw-Hill, New York (1937).
21. J. H. Seinfeld, *Atmospheric Chemistry and Physics of Air Pollution.* Wiley, New York (1986).
22. G. Doetsch, *Guide to the Applications of the Laplace and Z-Transforms* (2nd Edn). Van Nostrand Reinhold, London (1971).

APPENDIX. SOLUTION FOR INTERNAL CONCENTRATION PROFILE

The definitions of the symbols used most frequently are given in the Nomenclature.

Consider a spherically symmetric diffusion equation

$$\frac{\partial rC}{\partial t} = D_l \frac{\partial^2 rC}{\partial r^2}, \quad r < a$$
$$C = C_s, \qquad r = a \tag{A1}$$

with the initial values

$$C = f_0 + \frac{a}{r}\sum_{n=1}^{\infty} f_n \sin(rs_n/a), \quad t = 0,\ r < a$$
$$C_s = C_v, \qquad t = 0 \tag{A2}$$

where s_n is the nth positive non-zero root of

$$s \cot s = 1 + \frac{\alpha s^2}{3} \tag{A3}$$

where α is the constant parameter.

For convenience, we define the following dimensionless variables:

$$\frac{r}{a} \equiv R, \quad \frac{Dt}{a^2} \equiv \tau, \quad \frac{rC}{aC_v} \equiv u, \quad \frac{C_s}{C_v} \equiv u_s. \tag{A4}$$

Then the previous equations (A1) and (A2) are

$$\frac{\partial u}{\partial \tau} = \frac{\partial^2 u}{\partial R^2}$$
$$u = u_s, \qquad R = 1$$
$$u = \frac{f_0 R}{C_v} + \sum_{n=1}^{\infty} \frac{f_n \sin(Rs_n)}{C_v}, \quad \tau = 0$$
$$u_s = 1, \qquad \tau = 0. \tag{A5}$$

Applying the Laplace transform

$$U(P) = \int_0^{\infty} \exp(-Pt)u(t)\,dt \tag{A6}$$

these equations transform into

$$\frac{\partial^2 U}{\partial R^2} = -s^2 U - \frac{f_0 R}{C_v} - \sum_{n=1}^{\infty} \frac{f_n \sin(Rs_n)}{C_v} \tag{A7}$$

where for convenience $-s^2 \equiv P$. The solution of this equation is easily found to be

$$U = A \sin(Rs) - \frac{f_0 R}{s^2 C_v} + \sum_{n=1}^{\infty} \frac{B_n f_n \sin(Rs_n)}{C_v} \tag{A8}$$

where A and B_n are constants of integration.

By substituting this for equation (A7) the constants B_n are found to be

$$B_n = \frac{1}{-s^2 + s_n^2}. \tag{A9}$$

The constant A can be determined using the equation for the total mass of solute

$$M = \int_0^a 4\pi r^2 C \, dr + V_s C_s. \tag{A10}$$

Applying the Laplace transform and using definitions (A4) this is transformed to

$$\frac{M}{s^2 4\pi a^3 C_v} = -\int_0^1 RU \, dR - \frac{\alpha_s U(R=1)}{3} \tag{A11}$$

where the parameter α_s is the ratio of the volume of the solution and the droplet

$$\alpha = \frac{V_s}{4\pi a^3/3}. \tag{A12}$$

By substituting the general solution (A8) for the above equation and using the relationships (A3) and (A9), the integration constant A is found to be

$$A = \frac{\dfrac{f_0(\alpha_s+1)}{3C_v} - \dfrac{M}{4\pi a^3 C_v}}{\left(\sin s - s\cos s + \dfrac{\alpha_s s^2 \sin s}{3}\right)} + \sum_{n=1}^{\infty} \frac{f_n(\alpha-\alpha_s)s^2 \sin s_n}{3C_v(s^2-s_n^2)\left(\sin s - s\cos s + \dfrac{\alpha_s s^2 \sin s}{3}\right)}. \tag{A13}$$

In order to carry out the inverse transformation, we expand the solution (equation (A8) with integration constants (A9) and (A13)) in partial fractions. If any function $g(P)/G(P)$ has a simple pole at zero (i.e. at the limit $P \to 0$ the function $P(g(P)/G(P))$ has a non-zero, finite value), it can be expanded in the form [22]

$$\frac{g(P)}{G(P)} = \frac{g(P)}{P\dfrac{G(P)}{P}} = \frac{1}{P}\lim_{P\to 0}\left(\frac{g(P)}{\dfrac{G(P)}{P}}\right) + \sum_{n=1}^{\infty} \frac{g(P_n)}{P_n\left(\dfrac{d}{dP}\left(\dfrac{G(P)}{P}\right)\right)_{P=P_n}} \frac{1}{P-P_n} \tag{A14}$$

where the constants P_n are the simple, non-zero poles of $g(P)/G(P)$. This formula is known as Heaviside's expansion theorem. To avoid the tedious second term (the infinite series) in the expression (A13), we assume that the volume ratio parameters have the same values ($\alpha_s = \alpha$).

Now the first term in equation (A8) has a simple pole at zero in respect to variable P, and according to equations (A3) and (A14) the solution can be written in the form

$$U = \frac{MR}{\left(\dfrac{4\pi a^3}{3} + V_s\right)C_v}\frac{1}{P} + \sum_{n=1}^{\infty}\left[\frac{2\left(\dfrac{M}{V_s} - \dfrac{(\alpha+1)f_0}{\alpha}\right)}{\left(\dfrac{3(\alpha+1)}{\alpha} + \dfrac{\alpha s_n^2}{3}\right)\sin s_n} + f_n\right] \times \frac{\sin\left(\dfrac{rs_n}{a}\right)}{C_v}\frac{1}{P+s_n^2}. \tag{A15}$$

Note that s_n is only the positive root of equation (A3) although there are also negative roots. We have had to omit the negative roots because the solution was expanded in respect to P and both positive and negative roots correspond to the same value of P_n ($-s^2 \equiv p$).

The inverse transformation can be easily carried out using a transformation table (e.g. ref. [22]). Noting the definitions (A4) the final concentration profile is

$$C = \frac{M}{\dfrac{4\pi a^3}{3} + V_s} + \sum_{n=1}^{\infty}\left[\frac{2\left(\dfrac{M}{V_s} - \dfrac{(\alpha+1)f_0}{\alpha}\right)}{\left(\dfrac{3(\alpha+1)}{\alpha} + \dfrac{\alpha s_n^2}{3}\right)\sin s_n} + f_n\right]\frac{a}{r} \times \exp\left(\frac{-s_n^2 D_1 t}{a^2}\right)\sin\left(\frac{rs_n}{a}\right). \tag{A16}$$